Study for Temperature Coefficient of Frequency of Surface Acoustic Wave Devices with SiO_xN_y Film Using $LiTaO_3$ Substrate

A. Nishimura, S. Matsuda, Y. Kabe, and H. Nakamura
Skyworks Solutions, Inc.
Osaka, Japan
Atsushi.Nishimura@skyworksinc.com

***Abstract*— The dielectric film formed as a passivation film on the Interdigital Transducer (IDT) electrode of the Surface Acoustic Wave (SAW) device affects the frequency and the Temperature Coefficient of Frequency (*TCF*) of the SAW device. Since it is known that the sound velocity and Temperature Coefficient of Velocity (*TCV*) of the SiO_xN_y film have a correlation with its own refractive index, we fabricated a one-port resonator with dielectric films with different refractive indexes deposited respectively on IDT electrodes and we investigated whether it is possible to control the frequency and *TCF* of the one-port resonator by manipulating the refractive index of the dielectric film. This study uncovered that the *TCF* of the one-port resonator, as well as the resonant frequency, correlates with the refractive index of the dielectric film deposited on the IDT electrode. Here, it is considered that the behavior of the resonant frequency and *TCF* of the one-port resonator are influenced by the sound velocity and *TCV* of the dielectric film deposited on the IDT electrode and the SAW energy distribution.**

Keywords*— Interdigital Transducer (IDT), Temperature Coefficient of Frequency (TCF), Temperature Coefficient of Velocity (TCV), Surface Acoustic Wave (SAW), Silicon oxynitride (SiO_xN_y), $LiTaO_3$

I. Introduction

Surface acoustic wave (SAW) devices are increasing in demand in recent years since multiband systems have continued to grow as a capacity and speed in mobile phone communication systems increase. With this background, studies of SiO_2 film or Si_3N_4 film for passivation on the SAW devices have been actively conducted. In particular, the SiO_2 film has been actively studied to improve the frequency response and temperature coefficient of frequency (*TCF*) of SAW devices [1, 2, 3, 4]. The reason why research studies on the SiO_2 film have been actively conducted is that the SiO_2 film has *TCF* whereby positive and negative are different from those of the substrate materials. Therefore, when it is necessary to improve the *TCF* of the SAW devices, the SiO_2 film for passivation is better than the Si_3N_4 film, which has the same sign of *TCF* as the substrate materials.

The SiO_2 film or the Si_3N_4 film as the passivation film is necessary for protecting the SAW devices, however SAW devices themselves often suffer from the passivation film formation process that affects the frequency and *TCF*. Here, it is reported that the sound velocity and *TCV* of the SiO_xN_y film correlate with its refractive index [5, 6]. When SiO_xN_y film is used as a passivation film, it is expected that the frequency and *TCF* can be controlled by manipulating the refractive index. Since refractive index is a physical quantity that can be easily measured in mass production, the correlation between the refractive index and the frequency response of the SAW devices contributes to the control of the frequency and *TCF* with high accuracy. In the previous research reports, the authors uncovered the correlation between the frequency of the one-port resonators and the refractive index of the SiO_xN_y films [7, 8]. In this study, the correlation between the *TCF* of the one-port resonators and the refractive index of the SiO_xN_y films is investigated.

II. Experimental Methods

We fabricated a one-port resonator and measured its resonant frequency (f_r) and its *TCF*. The one-port resonator was fabricated with or without a dielectric film deposition on an IDT electrode. Here, each dielectric film of SiO_2, SiO_xN_y or Si_3N_4 was deposited and the refractive index was varied for each film. The *TCF* was estimated from the resonant frequency.

One-port resonators were fabricated by forming an IDT electrode with Al on a 42°*Y-X* $LiTaO_3$ substrate. Then, a dielectric film of SiO_2, SiO_xN_y or Si_3N_4 with each refractive index in the range as shown on Table I was deposited. The refractive indexes shown on Table I were measured by spectroscopic ellipsometry in this experiment. The measured refractive indexes of SiO_2 or Si_3N_4 films deposited in this experiment were similar to those in the previous research reports [9, 10].

A reactive RF sputtering system with a Si target was utilized to form a dielectric film at room temperature under the condition that the RF power density was 28 kW/m^2 and the pressure was 0.15 Pa. SiO_2 and Si_3N_4 films were respectively formed in Ar/O_2 and Ar/N_2 atmospheres, while SiO_xN_y films were formed in an $Ar/N_2/O_2$ atmosphere. The SiO_xN_y composition was modulated by changing the O2/N2 gas flow ratio from 0.25 to 0.40. The deposition rate was approximately 0.1 nm/s under all conditions.

The content ratio of oxygen [$x/(x+y)$] or nitrogen [$y/(x+y)$] in SiO_xN_y films in Table I was calculated by putting the obtained data of refractive indexes of SiO_xN_y films in a proportional equation that was given by the assumption that the content ratio of N in the SiO_2 film is 0% and that in the Si_3N_4 film is 100%.

Table II shows λ of one-port resonators, the relative thickness of the IDT electrode, and the relative thickness of the dielectric film. The f_r and *TCF* of three types of one-port

XXX-X-XXXX-XXXX-X/XX/$XX.00 ©20XX IEEE

Table. I Split Table for One-port Resonator Evaluation.

Split	Dielectric	Refractive index at 633 nm	$x/(x+y)$ %	$y/(x+y)$ %
(A)	SiO_2	1.478	100	0
(B)	SiO_xN_y	1.553	86.2	13.8
(C)	SiO_xN_y	1.618	74.2	25.8
(D)	SiO_xN_y	1.706	57.9	42.1
(E)	Si_3N_4	2.020	0	100
(F)	N/A	N/A	N/A	N/A

Table. II λ of One-port Resonator and Relative Thickness of IDT or Dielectric.

	IDT λ (μm)	Al thickness (h_{IDT}/λ)	Dielectric thickness ($h_{dielectric}/\lambda$)
Resonator A	1.9	0.042	0.26
Resonator B	2.0	0.040	0.25
Resonator C	2.1	0.038	0.24

resonators, which have different relative thicknesses of the IDT electrode and dielectric, was measured.

Next, the SAW energy distribution of the frequency response was simulated using Finite Element Method Spectral Domain Analysis (FEMSDA) [11, 12, 13]. This simulation result includes some consideration from our experimental results. The material constants of SiO_2 or Si_3N_4 that authors applied in the previous research [8] were used in this simulation. On the other hand, we used the material constant of the SiO_xN_y that is calculated using the constants of SiO_2 and Si_3N_4. The calculation was carried out assuming that the proportional expression of the content ratio of oxygen to nitrogen in Table I can be used.

III. Results and Discussion

Figure 1 shows the *Y(1,1)* admittance of the one-port resonators with λ=2.0μm. This data includes the cases of SiO_2, Si_3N_4 or SiO_xN_y films with different refractive indexes deposited on the IDT electrode, and also includes the case of no dielectric film is deposited on the IDT electrode. The frequency of the sample (A) for which the SiO_2 film was deposited on the IDT electrode was lower than that of the sample (F) with no dielectric film on the IDT electrode. The frequency of the sample (E) with the Si_3N_4 film deposited on the IDT electrode was higher than that of the sample (F). On the other hand, the resonant frequency of the SiO_xN_y films deposited on the IDT electrode (B, C, D) takes a value in the middle between the sample (A) with SiO_2 film deposition and the sample (E) with Si_3N_4 film deposition. It was also confirmed that the resonant frequency with SiO_xN_y films increases as the refractive index of SiO_xN_y film increases.

Figure 2 shows the shift of the resonant frequency of the one-port resonator in the case of depositing SiO_2, Si_3N_4 and SiO_xN_y films with different refractive index on the IDT electrode respectively, compared with the case of depositing no dielectric film on the IDT electrode. This graph shows the refractive index dependence of the frequency shift in each one-port resonator of λ = 1.9, 2.0 and 2.1μm. In Fig. 2, it can

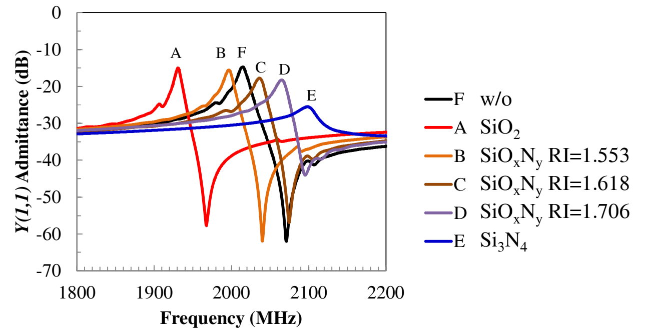

Fig. 1. Frequency response of one-port resonators with λ=2.0μm.

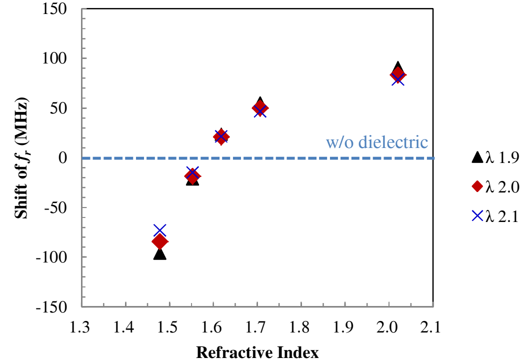

Fig. 2. Shift of resonant frequency (f_r) caused by dielectric deposition as a function of refractive index.

be seen that the shift in the resonant frequency has a correlation with the refractive index of the dielectric film deposited on the IDT electrode in each one-port resonator. Compared with the frequency of resonators with no dielectric film, the frequency of resonators with the SiO_2 film (refractive index 1.478) decreases and the frequency of the resonators with the Si_3N_4 film (refractive index 2.020) increases with any of the resonators at λ=1.9-2.1μm.

The frequency of resonators with the SiO_xN_y film changes as the refractive index of the SiO_xN_y film changes. Here, the change in the shift of the resonant frequency is large comparing with change of refractive index when the refractive index of the dielectric film on the IDT electrode closes to that of the SiO_2 film. On the other hand, the change in the shift of the resonant frequency is small comparing with the change of the refractive index when the refractive index of the dielectric film on the IDT electrode closes to that of the Si_3N_4 film.

Next, Fig. 3 shows *TCF* as a function of λ of the one-port resonators. This data includes the case of SiO_2, Si_3N_4 or SiO_xN_y film with different indexes deposited on the IDT electrode, and the case of the no dielectric film deposited on the IDT electrode. Fig. 4 also shows the dependence of the refractive index of the dielectric film deposited on the IDT electrode on the *TCF* of the one-port resonators.

It was confirmed that compared to the IDT electrode without dielectric film deposition, the *TCF* shifts to the plus side when the SiO_2 film is deposited on the IDT electrode whereas it shifts to the minus side when the Si_3N_4 film is

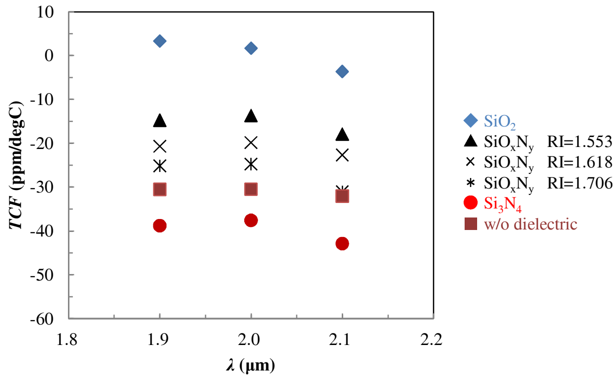

Fig. 3. *TCF* in the each of dielectric film deposition on the IDT electrode as a function of λ of the one-port resonators.

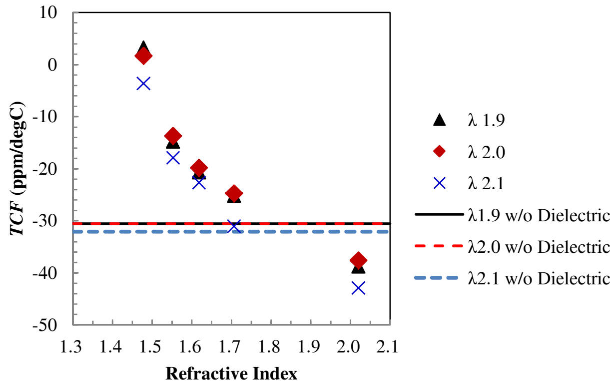

Fig. 4. *TCF* of the one-port resonators with the dielectric film on the IDT electrode as a function of refractive index.

deposited on the IDT electrode. This behavior was observed individually when λ = 1.9, 2.0, or 2.1 as shown on the Fig. 3. Fig. 3 also uncovers that the *TCF* of the one-port resonators shifts from the SiO_2 film side to the Si_3N_4 film side as the refractive index of the SiO_xN_y film increases.

In Fig. 4, it can be seen that the *TCF* of the one-port resonators correlates with the refractive index of the dielectric film deposited on the IDT electrode. Here, in each λ = 1.9, 2.0, 2.1μm on Fig. 4, the change in the *TCF* of the one-port resonators is large comparing with the change of the refractive index when the refractive index of the dielectric film on the IDT electrode closes to that of the SiO_2 film. And the change in *TCF* of the one-port resonators is small comparing with the change of the refractive index when the refractive index of the dielectric film on the IDT electrode closes to that of Si_3N_4 film. This behavior of the *TCF* is consistent with the correlation of the *TCV* of dielectric bulk films with the refractive index of dielectric films [5, 6]. Therefore this phenomenon in Fig. 4 is considered to reflect the effect of the *TCV* of the each dielectric films deposited on the IDT electrode. Here, we also found that if SiO_xN_y is used as a passivation film, the *TCF* turns to the plus side by making the refractive index of the SiO_xN_y film less than around 1.7.

Next, the simulation for the SAW energy distribution was conducted by FEMSDA in order to consider the resonant frequency and the *TCF* behaviors of the one-port resonator with the dielectric film deposited on the IDT electrode. Fig. 5 shows the cross-sectional structure set for the FEMSDA simulation and Fig. 6 shows the results of the simulation for the SAW energy distribution. Following the previous research studies [8], it was assumed that the dielectric film is deposited with the relative thickness shown in Table II on both of the IDT electrode and the $LiTaO_3$ substrate in this simulation. And this simulation is conducted with λ = 2.0 μm of the IDT electrode.

Here, the material constants of SiO_2 and Si_3N_4 are as follows in this simulation. The densities of SiO_2 and Si_3N_4 on the FEMSDA simulation are calculated using the measured refractive index on Table I. This procedure for calculation followed that the previous research studies [9]. For the Young's modulus, the values obtained in our previous study [8] were used. And we use the dielectric constants and the Poisson's ratio which is reported in the previous research studies [14, 15, 16]. On the other hand, the material constant of SiO_xN_y is as follows. The material constant of the SiO_xN_y film is calculated using the constant of SiO_2 and Si_3N_4. The calculation was carried out assuming that the proportional expression of the content ratio of oxygen to nitrogen in Table I can be used.

Figure 6 shows the SAW energy distribution resulting from FEMSDA calculation. The horizontal axis represents the amount of displacement in the shear horizontal (SH) direction directly under the IDT electrode. The displacement value is normalized by the amplitude of the displacement vector on the $LiTaO_3$ substrate surface. The vertical axis represents the distance that is normalized by the wavelength λ with the surface of the $LiTaO_3$ substrate being zero.

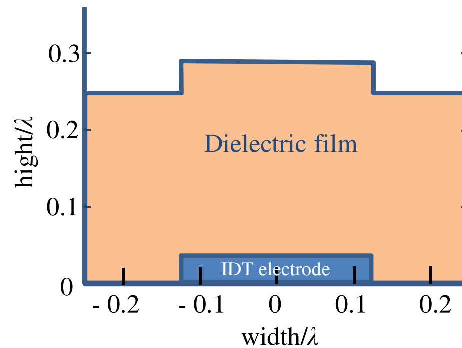

Fig. 5. Cross-sectional structure set for the FEMSDA simulation.

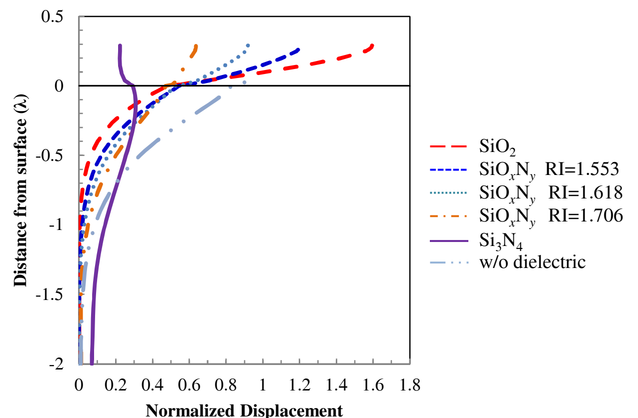

Fig. 6. SAW energy distribution in shear horizontal direction simulated using FEMSDA.

As shown in Fig. 6, the SAW energy distribution shifted toward the upper the dielectric film side when the dielectric film is formed on the IDT electrode comparing with the case of no dielectric deposition on the IDT electrode. Therefore, this behavior of the resonant frequency and the *TCF* of the one-port resonators are considered to reflect the effect of the velocity and the *TCV* of the each dielectric films deposited on the IDT electrode.

Here, it is confirmed that as the refractive index of the dielectric film deposited on the IDT electrode come close to the Si_3N_4 side from the SiO_2 side, the SAW energy distribution shifts to the $LiTaO_3$ substrate side. This may indicate that the resonant frequency and the *TCF* of the one-port resonators are less likely to be affected by the velocity and the *TCV* of the each dielectric film deposited on the IDT electrode. We consider this can be one of the reasons why the change of the resonant frequency shift and the change of the *TCF* decrease as the refractive index increases in Fig. 2 and Fig. 4.

IV. SUMMARY

In this study, the one-port resonators with the IDT electrode made of Al using the 42°*Y-X* $LiTaO_3$ substrate were fabricated, and the SiO_2 film, Si_3N_4 film or SiO_xN_y film with different refractive index were deposited on the IDT electrode. Here, we investigated the correlation between the *TCF* of the one-port resonators and the refractive index of the each dielectric films deposited on the IDT electrode and observed the following findings.

The data in this study demonstrated that compared to the IDT electrode without dielectric film deposition, the *TCF* shifts to the plus side when SiO_2 film is deposited on the IDT electrode whereas it shifts to minus side when Si_3N_4 film is deposited on the IDT electrode. The data also demonstrated that the *TCF* of the one-port resonators as well as the resonant frequency of the one-port resonators correlated with the refractive index of the dielectric film on the IDT electrode.

Our data also demonstrated that the change in the *TCF* of the one-port resonators is large when the refractive index of the dielectric film on the IDT electrode is close to that of the SiO_2 film, on the other hand the change in the *TCF* of the one-port resonators is small when the refractive index of the dielectric film on the IDT electrode is close to that of the Si_3N_4 film. This behavior of the *TCF* is consistent with the previous research studies [5, 6] which report the correlation of the *TCV* of dielectric bulk films with the refractive index of the dielectric films. Therefore, the phenomenon in this experiment is considered to reflect the effect of the *TCV* of the each dielectric films deposited on the IDT electrode.

Moreover, the simulation using FEMSDA suggested that the SAW energy distribution is one of the factors influencing the behavior of the *TCF* of the each one-port resonators.

This study tells us that the managing the refractive indexes of the SiO_xN_y films can apply to the adjustment of not only the resonant frequency but also the *TCF*. In conclusion, we suggest that it is useful to adjust the refractive index of SiO_xN_y film to control the property of SAW devices.

REFERENCES

[1] K. Asai, M. Hikata, A. Isobe, K. Sakiyama, and T. Tada, Proc. IEEE Ultrasonics Symp., 2002, p. 235.

[2] M. Kadota, T. Nakao, N. Taniguchi, E. Tanaka, M. Miura, K. Nishiyama, T. Hada, and T. Komura, Proc. IEEE Ultrasonics Symp., 2003, p. 2105.

[3] M. Kadota, T. Nakao, N. Taniguchi, E. Tanaka, M. Miura, K. Nishiyama, T. Hada, and T. Komura, Proc. IEEE Int. Ultrasonics, Ferroelectrics, and Frequency Control Joint 50th Anniversary Conf., 2004, p. 1970.

[4] M. Kadota, T. Nakao, N. Taniguchi, E. Takata, M. Miura, K. Nishiyama, T. Hada, and T. Komura, Jpn. J. Appl. Phys. **44**, 4527 (2005).

[5] S. Tsuboi, H. Ogi, A. Nagakubo, M. Hirao, S. Matsuda, and Y. Kabe, presented at 72nd Spring Meet. Physical Society of Japan, 2017, 17pC43-4 [in Japanese].

[6] S. Tsuboi, H. Ogi, A. Nagakubo, N. Nakamura, S. Matsuda, and Y. Kabe, presented at IEEE Ultrasonics Symp., 2017, P4-A2-1.

[7] A. Nishimura, S. Matsuda, Y. Kabe, and H. Nakamura, Proc. Symp. Ultrasonic Electronics, 2017, 1J3-1.

[8] A. Nishimura, S. Matsuda, Y. Kabe, and H. Nakamura, Jpn. J. Appl. Phys. **57**, 07LD23 (2018).

[9] T. Baak, Appl. Opt. **21**, 1069 (1982).

[10] A. Nagakubo, H. Ogi, H. Ishida, M. Hirao, T. Yokoyama, and T. Nishihara, J. Appl. Phys. **118**, 014307 (2015).

[11] K. Hashimoto, G. Q. Zheng, and M. Yamaguchi, Proc. IEEE Ultrasonics Symp., 1997, p. 279.

[12] K. Hashimoto, T. Omori, and M. Yamaguchi, Int. Frequency Control Symp. Exhib., 2000, p. 307.

[13] K. Hashimoto, T. Omori, and M. Yamaguchi, Proc. IEEE Ultrasonics Symp., 2007, p. 711.

[14] Nihon Gakujutsu Shinkokai Danseiha Soshi Gijutsu Dai 150 Iinkai, Danseiha Soshi Gijutsu Handbook (Ohmsha, Tokyo, 1991) p. 320 [in Japanese].

[15] Y. Matsumura, and Y. C. Huang, Nihon Kinzoku Gakkaishi 47, 991 (1983) [in Japanese].

[16] Y. Yoshioka, K. Akita, and H. Suzuki, Nihon Kinzoku Gakkaishi 50, 690 (2001) [in Japanese].